Journal of Engineering Physics and Thermophysics, Vol. 72, No. 5, 1999

CALCULATION OF RADIATIVE TRANSFER IN NONGRAY GAS USING A NARROW-BAND MODEL AND MONTE CARLO SIMULATION

M. Cherkaoui, M. Asbik, and A. Khmou

UDC 621.039.51

Radiation transfer is treated by the application of a narrow-band statistical model (NBSM) that takes emission and absorption gas spectral structures into account. A Monte Carlo method (MCM) using a net exchange technique was developed to integrate the radiative-transfer equation in nongray gas. The proposed procedure is based on a net-exchange formulation (NEF). This formulation provides an efficient way of systematically fulfilling the reciprocity principle, which avoids some of the major problems usually associated with the Monte Carlo method; the numerical efficiency becomes independent of the optical thickness, highly nonuniform grid sizes can be used with no increase in computation time, and configurations with small temperature differences can be treated with very good accuracy. It is shown that the radiative term is significant compared to the conductive term in just two specific regions in the emitting and absorbing gas in the immediate vicinity of the wall and in the external part of the boundary layer. The exchange Monte Carlo method (EMCM) is described in detail for a one-dimensional slab.

1. INTRODUCTION

Radiative heat transfer arises in many engineering devices (solar-energy systems, atmospheric systems, combustion systems, nuclear reactors, etc.). The present study is devoted to the development of a rather precise method for radiation exchange computations in an air/water vapor or air/carbon dioxide mixture.

Numerical simulations of radiative heat transfer in gases arose mainly in meteorology and astrophysics research [1] and in engineering heat-transfer research on high-temperature systems [2]. These efforts concerned the development of gas radiation models and their implementation in complete radiative heat transfer simulations through integration of the radiative equation. Nowadays the use of exact line-by-line models remains unfeasible for complex systems. Most earlier authors used a gray gas assumption [3-5], and optically thin [6, 7] and thick [3, 4, 6] limits were also frequently considered. Cess [7] treated a nongray gas for which the absorption coefficient, depending on the wavelength, was assumed to be independent of temperature. Novotny et al. [8] formulated the radiative term using the total band absorption based on an exponential wide-band model. However, there are more accurate radiative models such as the exponential wide-band model [9, 10], the random-statistics narrow-band model proposed by Malkmus in 1967 [11], and the model of Soufiani et al. [12]. This type of model has been applied more frequently to an emitting and absorbing medium.

We will not enter into a detailed description of the use the MCM with the NBSM; one may also refer to works of Cherkaoui [13] and Liu et al. [14].

2. BASIC FORMULATION

We consider an emitting, absorbing, and nonscattering gas with the temperature profile $T(y)$ between two vertical plates at the temperatures T_{w1} and T_{w2} respectively. Here the emissivities ε_1 and $\varepsilon_2 = 1$ (see Fig. 1). The following assumptions are made:

Département de Physique, Faculté des Sciences et Techniques, Errachidia, Morrocco; Département de Physique, Faculté des Sciences, Meknes, Morrocco. Published in Inzhenerno-Fizicheskii Zhurnal, Vol. 72, No. 5, pp. 937-945, September-October, 1999. Original article submitted January 25, 1998.

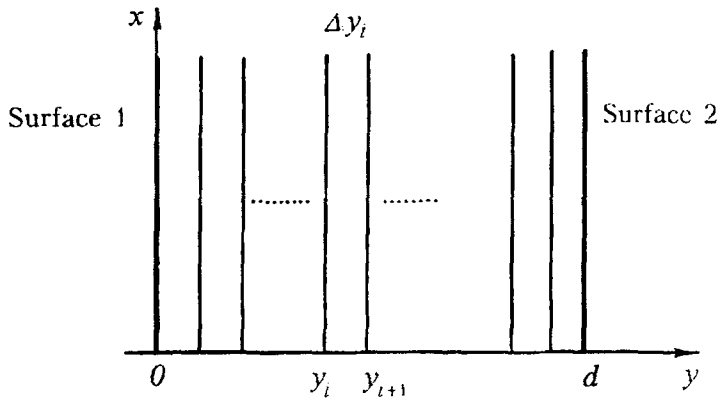

Fig. 1. System coordinates and spatial discretization.

- the gas has constant physical properties;
- the radiative dissipation in the x-direction is negligible in comparison with that in the y-direction;
- the surfaces are black.

2.1. Monochromatic Formulation. The radiative flux per unit area in the y direction is [13]

$$\vec{q}^{\,R} = 2\pi \int_0^{+\infty} d\nu \left[\int_0^{1} I_\nu \mu d\mu - \int_0^{-1} I_\nu \mu d\mu \right]; \tag{1}$$

$$I_\nu (y) = I_\nu (0)\, \tau_\nu (0, y, \mu) + \int_0^{y} I_\nu^{b} (y') \frac{\partial \tau_\nu (y', y, \mu)}{\partial y'} dy'. \tag{2}$$

The local radiative balance at infinite volume of the gas at y is [13]

$$\frac{\partial \psi_\nu^{g}}{\partial y} = 2\pi \left(I_\nu^{b} (T_{w1}) - I_\nu^{b} (T(y))\right) \int_0^{1} \frac{\partial \tau_\nu (0, y, \mu)}{\partial y} d\mu + 2\pi \left(I_\nu^{b} (T_{w2}) - \right.$$

$$\left. - I_\nu^{b} (T(y))\right) \int_0^{1} \frac{\partial \tau_\nu (d, y, \mu)}{\partial y} d\mu +$$

$$+ 2\pi \int_0^{d} k_\nu \left(I_\nu^{b} (T(y')) - I_\nu^{b} (T(y))\right) dy' \int_0^{1} \frac{\partial^2 \tau_\nu (d, y, \mu)}{\partial y' \partial y} d\mu; \tag{3}$$

$$\frac{\partial \psi_\nu^{g}}{\partial y} = \frac{\partial \psi_\nu^{gw1} (y, 0)}{\partial y} + \frac{\partial \psi_\nu^{gw2} (y, d)}{\partial y} + \int_0^{d} \frac{\partial^2 \psi_\nu^{gg} (y, y')}{\partial y' \partial y} dy'. \tag{4}$$

The net-exchange rate (NER) between two elementary gas layers at coordinates y and y' is defined by

$$\frac{\partial^2 \psi_\nu^{gg}}{\partial y \partial y'} = 2\pi \left(I_\nu^{b} (T(y')) - I_\nu^{b} (T(y))\right) \int_0^{1} \frac{\partial^2 \tau_\nu (d, y, \mu)}{\partial y \partial y'} \mu d\mu = - \frac{\partial^2 \psi_\nu^{gg}}{\partial y' \partial y}. \tag{5}$$

The net-exchange rate between surface m ($m = 1$ or 2) and the elementary gas layer at y is

$$\frac{\partial \psi_\nu^{gs} (y, m)}{\partial y} = \pi \left(I_\nu^{b} (T_{wm}) - I_\nu^{b} (T(y))\right) \int_0^{1} \frac{\partial \tau_\nu (0, y, \mu)}{\partial y} d\mu = - \frac{\partial \psi_\nu^{sg} (y, m)}{\partial y}. \tag{6}$$

And the net-exchange rate between the two surfaces is

$$\psi_\nu^{ss}(1,2) = 2\pi\left(I_\nu^b(T_{w1}) - I_\nu^b(T_{w2})\right)\int_0^1 \tau_\nu(0,d,\mu)\,d\mu = -\psi_\nu^{ss}(2,1)\,. \tag{7}$$

Local radiation balances may be expressed using partial exchanges. The resulting expression for the net inflow at y of monochromatic radiant energy per unit volume is:

$$\frac{\partial\psi_\nu^g(y)}{\partial y} = \int_0^d \frac{\partial^2\psi_\nu^{gg}(y,y')}{\partial y\partial y'}\,dy' + \sum_{m=1}^{2}\frac{\partial\psi_\nu^{gs}(y,m)}{\partial y}\,. \tag{8}$$

The radiation balance for surface 1 is

$$\psi_\nu^s(1) = \int_0^d \frac{\partial\psi_\nu^{sg}(1,y')}{\partial y'}\,dy' + \psi_\nu^{ss}(1,2)\,. \tag{9}$$

2.2. Radiative Model. Approximations for the transmissivity τ_ν, averaged over $\Delta\nu$, of a column of length L at temperature T, total pressure P, and mole fraction x of the absorbing species are presented.

The box model was first developed by Penner [15] with the smeared-rotational-line-model approach; it assumes that the spectral absorption coefficient k_ν is constant inside $\Delta\nu$ and equal to

$$\bar{k} = \int_{\nu-\Delta\nu}^{\nu+\Delta\nu} k_\nu\,d\nu\,. \tag{10}$$

The low-resolution transmissivity is then given by

$$\bar{\tau}_{\Delta\nu} = \exp(-\bar{k}L)\,. \tag{11}$$

The narrow-band statistical model due to Goody [1] involves two approximations. The first assumes that the lines are randomly placed. The lines centered outside and inside $\Delta\nu$ are considered identical. The low-resolution transmissivity for the Lorentz shape is given by

$$\bar{\tau}_{\Delta\nu} = \exp\left(-\Delta\nu^{-1}\sum_{j=1}^{M} W_j\right) = \exp\left(-\Delta\nu^{-1}\sum 2\pi\gamma_j\,\mathrm{LR}\left(\frac{S_j xPL}{2\pi\gamma_j}\right)\right)\,. \tag{12}$$

For fast computations, LR is well approximated by [11]

$$\mathrm{LR}(z) = z\left[1 + \left(\frac{\pi z}{2}\right)^{1.25}\right]^{0.4}\,. \tag{13}$$

The second approximation assumes that the line intensities S_j obey a statistical distribution law $P(S)$. The most widely used relations will now be listed.

(i) The uniform distribution, which assumes that all lines have the same intensity and half-width, leads to [16]

$$\bar{\tau}_{\Delta\nu} = \exp\left(-\frac{2\pi\bar{\gamma}}{\delta}\,\mathrm{LR}\left(\frac{\bar{k}\,\delta xPL}{2\pi\bar{\gamma}}\right)\right)\,. \tag{14}$$

The mean parameters $\bar{k}$, $\bar{\delta}$, $\bar{\gamma}$ are [1, 17]

$$\bar{k} = \Delta\nu^{-1}\sum_{j=1}^{M} S_j\,; \tag{15}$$

$$\bar{\gamma} = M^{-1} \sum_{j=1}^{M} \gamma_j ; \tag{16}$$

$$\bar{\delta} = \frac{\bar{k}\,\bar{\gamma}}{\left(\Delta\nu^{-1} \sum_{j=1}^{M} \sqrt{S_j \gamma_j}\right)^2} . \tag{17}$$

(ii) The one-parameter exponential-tailed distribution is given by [1]

$$P(S) = \bar{S}^{-1} \exp\left(-\frac{S}{\bar{S}}\right) \tag{18}$$

and leads to

$$\bar{\tau}_{\Delta\nu} = \exp\left(-\frac{2\pi\,\bar{\gamma}}{\left(1 + \dfrac{\bar{k}\,\bar{\delta}\,xPL}{4\bar{\gamma}}\right)^{1/2}}\right) . \tag{19}$$

(iii) The two-parameter exponential-tailed-inverse distribution [13]

$$P(S) = \frac{1}{S \log r}\left[\exp\left(-\frac{S}{S_M}\right) - \exp\left(-\frac{rS}{S_M}\right)\right] \tag{20}$$

leads to

$$\bar{\tau}_{\Delta\nu} = \exp\left(-\frac{2\bar{\gamma}}{\bar{\delta}}\left(\left(1 + \frac{\bar{k}\,\bar{\delta}\,xPL}{\bar{\gamma}}\right)^{1/2} - 1\right)\right) . \tag{21}$$

Various narrow-band radiative models have been tested with line-by-line calculation for CO_2-air and H_2O-air mixtures [12]. The most accurate temperature and flux distributions are obtained with a narrow-band statistical model that assumes the absorption lines to be randomly placed and the intensities to obey an exponential-tailed-inverse distribution.

2.3. Radiation Balances in the NBSM. The preceding expressions can be integrated over a spectral width $\Delta\nu$. If the interval is narrow enough, the blackbody intensity can be assumed uniform. Integration of Eq. (5) gives, for instance,

$$\frac{\partial^2 \bar{\psi}_{\Delta\nu}^{gg}(y, y')}{\partial y \partial y'} = \frac{1}{\Delta\nu} \int_{\Delta\nu} \frac{\partial^2 \psi_\nu^{gg}(y, y')}{\partial y \partial y'}\, d\nu ,$$

$$\frac{\partial^2 \bar{\psi}_{\Delta\nu}^{gg}(y, y')}{\partial y \partial y'} = 2\pi \left(\bar{I}_{\Delta\nu}^{b}(T(y')) - \bar{I}_{\Delta\nu}^{b}(T(y))\right) \frac{1}{\Delta\nu} \int_{\Delta\nu} d\nu \int_0^1 \frac{\partial^2 \tau_\nu(d, y, \mu)}{\partial y \partial y'}\, \mu\, d\mu . \tag{22}$$

Inverting the frequency and angular integration leads to the following expression:

$$\frac{\partial^2 \bar{\psi}_{\Delta\nu}^{gg}(y, y')}{\partial y \partial y'} = 2\pi \left(\bar{I}_{\Delta\nu}^{b}(T(y')) - \bar{I}_{\Delta\nu}^{b}(T(y))\right) \int_0^1 \frac{\partial^2 \bar{\tau}_{\Delta\nu}(d, y, \mu)}{\partial y \partial y'}\, \mu\, d\mu \tag{23}$$

with

$$\bar{\tau}_{\Delta\nu}(y, y', \mu) = \exp\left(-\frac{2\bar{\gamma}}{\delta}\left(\left(1 + \frac{\bar{k}\,\delta\, xP\,|y - y'|}{\mu\bar{\gamma}}\right)^{1/2} - 1\right)\right). \tag{24}$$

The integration over the whole spectrum is obtained by adding the contributions of the N_b narrow bands:

$$\frac{\partial^2 \psi^{gg}(y, y')}{\partial y \partial y'} = \sum_{l=1}^{N_b} \frac{\partial^2 \psi_l^{gg}(y, y')}{\partial y \partial y'} \Delta\nu. \tag{25}$$

Similar expressions are obtained for the radiation balance of gas-surface and surface-surface exchanges.

2.4. Discretization. The volume of gas is divided into N_d layers of thickness Δy_i. We emphasize that the layers are not assumed isothermal; the internal-temperature profiles are accounted for without restriction. If we consider the i-th gas layer between the abscissas y_i and y_{i+1} and the j-th gas layer between y_j and y_{j+1}, Eq. (23) can be integrated over y and y' to give the average NER between layers i and j:

$$\bar{\psi}_{\Delta\nu}^{gg}(i, j) = 2\pi \int_{y_i}^{y_{i+1}} dy \int_{y_j}^{y_{j+1}} (\bar{I}_{\Delta\nu}^{b}(T(y')) - \bar{I}_{\Delta\nu}^{b}(T(y)))\, dy' \int_0^1 \frac{\partial^2 \bar{\tau}_{\Delta\nu}(y, y', \mu)}{\partial y \partial y'} \mu d\mu. \tag{26}$$

The average between layer i and surface 1 is given by

$$\bar{\psi}_{\Delta\nu}^{gs}(i, 1) = 2\pi \int_{y_i}^{y_{i+1}} (\bar{I}_{\Delta\nu}^{b}(T(y)) - \bar{I}_{\Delta\nu}^{b}(T_{w1}))\, dy \int_0^1 \frac{\partial \bar{\tau}_{\Delta\nu}(y, 0, \mu)}{\partial y} \mu d\mu. \tag{27}$$

An equivalent expression can be derived for $\bar{\psi}^{gs}(i, 2)$.

The average radiation budget for the i-th layer is

$$\bar{\psi}_l^{g}(i) = \sum_{j=1}^{N_d} \bar{\psi}_l^{gg}(i, j) + \sum_{m=1}^{2} \bar{\psi}_l^{gs}(i, m) \tag{28}$$

and for surface 1

$$\bar{\psi}_l^{s}(1) = \sum_{j=1}^{N_d} \bar{\psi}_l^{sg}(1, j) + \bar{\psi}_l^{ss}(1, 2). \tag{29}$$

3. THE MONTE CARLO METHOD

Radiative-transfer specialists commonly turn to the Monte Carlo method as a method for numerical simulation of a stochastic process; by invoking a probabilistic model of the radiative exchange process and applying Monte Carlo sampling techniques, it is possible to choose a semimacroscopic approach and avoid many difficulties inherent in the averaging process of the usual integral-equation formulation [18]. The aforementioned probabilistic model is usually designed in strict analogy with the physical processes of photon emission, transmission, and absorption. We will refer to such methods as analog Monte Carlo methods (AMCM).

The present approach is significantly different. We make use of the MCM for numerical computation of multidimensional integrals. No physical probabilistic model is required. An integral formulation is chosen (NEF) and a statistical method (MCM) is used to compute integrals. A major feature of this a method is that the sampling laws could be chosen arbitrarily and do not match any physical property.

3.1. Principle. The Monte Carlo procedure for numerical estimation of the integral

$$A = \int_D f(v)\, dv$$

is the following:

(i) A probability density function (pdf) $p(v)$ is chosen arbitrarily on D with the only constraint that it must be nonzero on D.

(ii) The associated weighting function is defined as

$$w(v) = \frac{f(v)}{p(v)}. \tag{30}$$

(iii) N values of v are generated randomly according to $p(v)$, and for each value the corresponding weighting factor w is computed. The average value нwo$_N$ and the variance $\sigma_N^2(w)$ of these N realizations of the variable $w(v)$ are computed. $\langle w\rangle_N$ and $\sigma_N^2(w)$ themselves are random variables.

(iv) $\tilde{A} = \langle w\rangle_N$ is an estimate of the integral A. The expectation of $\tilde{A}$ is A. An estimate of the standard deviation of $\tilde{A}$ (henceforth called the "statistical error") is

$$\tilde{\sigma}_N(\tilde{A}) = N^{-0.5}\,\sigma_N(w).$$

When computing sums instead of integrals, the preceding procedure is valid if the pdf's are replaced by discrete probabilities.

The key point of this method is the choice of the probabilities and the pdf. Again, this choice is a priori totally arbitrary. However, an improper choice of the probabilities may lead, for a prescribed precision, to an extremely large sampling size. Obviously, the criterion is the variance of $w(v)$. Thus one should choose $p(v)$ such that the variations of $f(v)/p(v)$ are minimal, keeping in mind that the random generation according to $p(v)$ must be feasible and computationally efficient. The probabilities may also be chosen to match physical properties (like the Lambert law for surface emission angles). This may lead to an increase in computational costs but provides the developer with a useful physical insight into the numerical procedure.

3.3. Probability Functions. The MCM is applied to compute the multidimensional integrals that appear in the NEF. In this formulation, independent expressions correspond to the NER for each pair of cells. It is therefore natural (although not necessary) to preserve this independence in the numerical scheme. We present here the probability functions retained for the MCM integration of the NER between two gas layers. For details one may refer to [13].

The total NER between the i-th and j-th gas layers is defined from Eq. (28):

$$\psi^{gg}(i,j) = \sum_{l=1}^{N_b} \Delta\nu \int_{y_i}^{y_{i+1}} dy \int_{y_j}^{y_{j+1}} dy' \int_0^1 f^{gg}(l, y, y', \mu)\, d\mu \tag{31}$$

with

$$f^{gg}(l, y, y', \mu) = 2\pi\,(\bar{I}_l^b(T(y')) - \bar{I}_l^b(T(y)))\,\mu\,\frac{\partial^2 \bar{\tau}_l(d, y, \mu)}{\partial y \partial y'}. \tag{32}$$

Thus the total NER computation involves one discrete sum, one integral over angles, and two integrals over the coordinates y and y'. According to the general procedure presented in the preceding paragraph, we need to define probabilities for each of these quantities. The associated weighting function will then can be can obtained from Eq. (30):

$$w_{ij}^{gg}(l, y, y', \mu) = \frac{f^{gg}(l, y, y', \mu)}{p(l)\,p_i(y)\,p_j(y')\,q(\mu)}. \tag{33}$$

3.3.1. Probability function for the positions y and y'. Uniform densities are used for positions within layers i and j given by

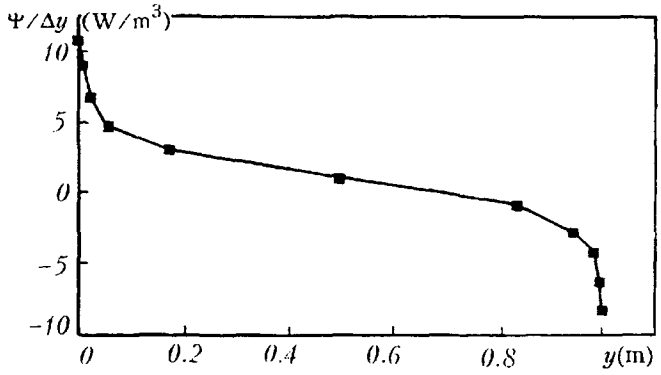

Fig. 2. Volumetric budget for pure carbon dioxide with a linear temperature profile varying from 305 K to 295 K and black surfaces.

TABLE 1. Function f to Be Integrated and the Chosen pdf for Surface-Surface, Surface-Gas and Gas-Gas Radiation Exchanges with Black Surfaces

ψ	f	$p_i(y)$	$p_i(y')$	$q(\mu)$	χ_l
$\psi^{ss}(1, 2)$	$f^{ss}(l, 0, d, \mu) = 2\pi(\bar{I}_l^b(T_{w1}) - \bar{I}_l^b(T_{w2}))\mu\bar{\tau}_l(0, d, \mu)$	–	–	2μ	$\frac{f^{ss}(l, 0, d, \tilde{\mu})}{q(\tilde{\mu})}$
$\psi^{gs}(i, m)$	$f^{gs}(l, y, y_w, \mu) = 2\pi(\bar{I}_l^b(T(y)) - \bar{I}_l^b(T(y_w))) \times \mu\partial\bar{\tau}_l(y, y_w, \mu)/\partial y$	$1/\Delta y_i$	–	1	$\frac{f^{gs}(l, \tilde{y}, y_w, \tilde{\mu})}{p_i(\tilde{y})q(\tilde{\mu})}$
$\psi^{gg}(i, j)$	$f^{gg}(l, y, y', \mu) = 2\pi(\bar{I}_l^b(T(y')) - \bar{I}_l^b(T(y)))\mu\partial^2\bar{\tau}_l(y, y', \mu)/\partial y\partial y'$	$1/\Delta y_i$		1	$\frac{f^{gg}(l, \tilde{y}, \tilde{y}', \tilde{\mu})}{p_i(\tilde{y})p_j(\tilde{y}')q(\tilde{\mu})}$

$$y = y_i + R\Delta y_i , \tag{34}$$

R is a random variable distributed uniformly in the interval [0, 1].

A similar expression gives the position y':

$$y' = y_j + R\Delta y_j . \tag{35}$$

3.3.2. Probability function for the direction. The direction cosine is given by an isotropic angular distribution:

$$\mu = R . \tag{36}$$

3.3.3. Probability for spectral bands. In order to determine discrete probabilities for spectral bands, we tried to estimate roughly the NER $\psi_l^{gg}(i, j)$ between i and j on each band l. This makes it possible to favor bands on which most of the radiative exchanges occur. If the pdf chosen for y, y', and μ are meaningful, one can simply state that if $\tilde{y}$, $\tilde{y}'$, and $\tilde{\mu}$ are the average values of y, y', and μ according to $p_i(y)$, $p_j(y')$, and $q(\mu)$, respectively, then a rough estimate of $\psi_l^{gg}(i, j)$ is

$$\chi_l^{gg}(i, j) = \frac{f^{gg}(l, \tilde{y}, \tilde{y}', \tilde{\mu})}{p_i(\tilde{y})\, p_j(\tilde{y}')\, q(\tilde{\mu})} . \tag{37}$$

Therefore the following probability is chosen for the l-th spectral band:

$$p(l) = \frac{|\chi_l|}{\sum_{k=1}^{N_b} |\chi_k|} . \tag{38}$$

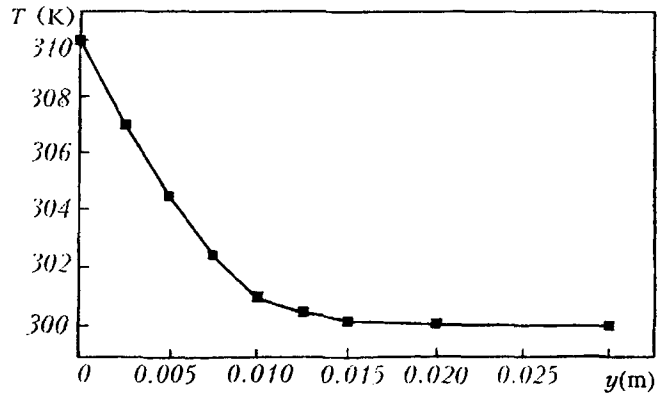

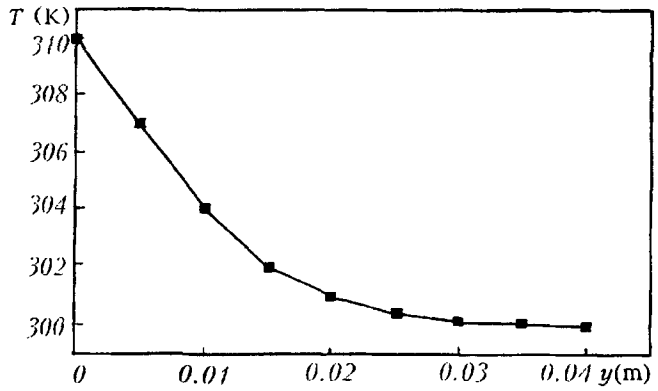

Fig. 3. Schmidt–Beckmann temperature profile in pure carbon dioxide ($x_{CO_2} = 1$).

Fig. 4. Comparison between net conductive exchange and net radiative exchange in pure carbon dioxide.

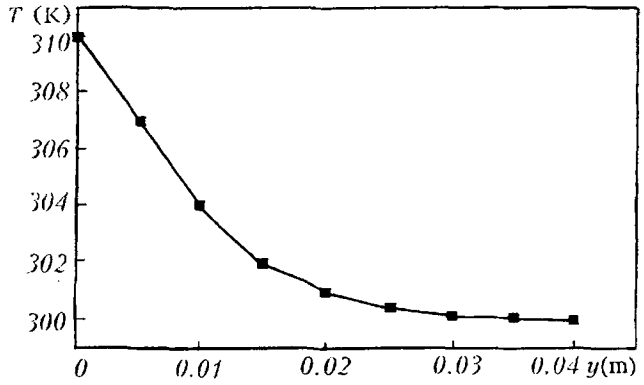

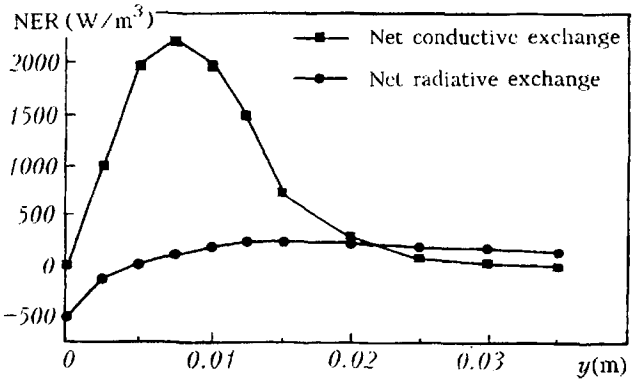

Fig. 5. Schmidt–Beckmann temperature profile in an air-water vapor mixture ($x_{H_2O} = 1.8 \cdot 10^{-2}$).

Fig. 6. Comparison between net conductive exchange and net radiative exchange in an air-water vapor mixture.

For the random generation of a spectral band according to the set of discrete probabilities $p(1)$, $p(2)$, ... $p(N_b)$, l is chosen as the solution of the following double inequality:

$$\sum_{k=1}^{l-1} p(k) < R < \sum_{k=1}^{l} p(k) . \tag{39}$$

Similar developments are required for gas-surface and surface-surface exchanges (Table 1).

4. RESULTS

4.1. Consistency of the Method for Nonuniform Discretization. Highly nonuniform discretizations introduce no specific convergence difficulties. Figure 2 displays volumetric radiation budgets in pure carbon dioxide. A strongly varied discretization is used in order to allow an accurate simulation of the large radiation budget gradients at the walls: 10 layers with sizes ranging from 2 mm to 10 cm and two zero-thickness layers enabling the computation of the limit value of the radiation budget at the boundaries. These profiles are typical examples of convergence qualities that would not be achievable with a standard AMCM at acceptable computational costs.

4.2. Estimation of Radiative Transfer in Natural Convection. Many authors have neglected the radiative term in natural convection owing to the fact that the problem becomes very complicated. This requires resolution

of the equation of natural convection coupled with the radiative-transfer equation, especially for radiative models that take emission and absorption gas spectral structures into account (e.g., line-by-line, MSBE). It is only recently, with the development of means and methods of calculation, that they have started to take into account the radiative effect. Here we give an estimate of this term from the theoretical temperature profile of Schmidt–Beckmann. And we are compare it with the conductive term.

Figure 3 presents a temperature profile of carbon dioxide at the vicinity of a hot vertical plate. This medium represents a strongly absorbing gas. Figure 4 presents a temperature profile of water vapor in the vicinity of a hot vertical plate. This medium represents a weakly absorbing gas. From these two profiles we determine the NER by the method and model described above. We will not enter into a detailed description of the calculation of the conductive term; one may also refer to [13]. We can make the following conclusions.

4.2.1. A strongly absorbing gas. The NER is not negligible compared to the conductive term in the immediate vicinity of and far from the hot wall in a strongly absorbing and emitting gas (Fig. 5). In the intermediate region, the NER rapidly becomes of secondary importance.

4.2.2. A weakly absorbing gas. In this case it turns out that the radiative effect can have a very important role in the immediate vicinity of the hot plate (Fig. 6). Beyond that it becomes insignificant.

This estimate of the radiative term in free convection shows that this term has an important effect mainly in the vicinity of and far from the hot plate. Thus the interaction of radiation and convection is significant, and it seems that a study of the coupled problem of radiation-convection in an emitting and absorbing gas is necessary.

NOTATION

A, integral to be estimated; d, distance between the two surfaces; D, spatial domain of integration; I^b, blackbody intensity; k, monochromatic absorption coefficient; $\bar{k}$, narrow-band average transmission coefficient; l, narrow-band index; L, length of the column; m, surface index; N, number of realizations; N_d, number of gas layers; N_b, number of narrow bands; P, pressure of the gas; p, probability; q, direction cosine probability density function; q^R, radiation heat flux; R, random variable distributed uniformly; r, ratio of the maximum and minimum values of the intensity within $\Delta\nu$; LR, Ladenburg–Reiche function [11]; M, number of lines centered within $\Delta\nu$; S, integrated intensity of the line; w, statistical weight; W, equivalent width; x, molar fraction; y, coordinate; y_i, abscissa of separation between the $(i-1)$-th and (i)-th gas layers; y_w, coordinate of the surface; $\tilde{y}$, abscissa of the center of layer (i); Δy, gas-layer thickness; $\Delta\nu$, wave-number interval; ν, wave number; γ, half-width; μ, cosine of the cone angle (measured from the normal to the surface); δ, equivalent line spacing; $\psi(i, j)$, energy net-exchange rate between (i) and (j), defined as the rate at which energy is emitted at (j) and absorbed at (i) minus the rate at which energy is emitted at (i) and absorbed at (j); $\psi(i)$, radiation budget of layer (i), W/m^2; τ, monochromatic transmission function; $\bar{\tau}_{\Delta\nu}$, Malkmus average transmission function; χ_l, rough estimate of $\bar{\psi}_l$; σ, standard deviation. Superscripts and subscripts: $(\bar{\ })_l$, average for narrow band l, index l is omitted when irrelevant; g, gas layer; gg, exchange between two gas layers; gs, exchange between a gas layer and an opaque surface; sg, exchange between an opaque surface and a gas layer; s, opaque surface; ss, exchange between two opaque surfaces; b, blackbody; M, maximum; ν, monochromatic quantity; w, wall (surface). Abbreviations: AMCM, analog Monte Carlo method; EMCM, exchange Monte Carlo method; MCM, Monte Carlo method; NEF, net-exchange formulation; NER, net-exchange rate; pdf, probability density function.

REFERENCES

1. R. M. Goody and Y. L. Yung, *Atmospheric Radiation*, 2nd edn., Oxford Univ. Press, U.K. (1989).
2. C. B. Ludwig, W. Malkmus, J. E. Reardon, and L. A. L. Thompson, *Handbook of Infrared Radiation from Combustion Gases*, NASA SP-3080 (1973).
3. R. D. Cess, *Int. J. Heat Mass Transfer*, **9**, 1269 (1966).
4. W. G. England and A. F. Emery, *J. Heat Transfer*, **91**, 37 (1969).
5. J. B. Bergquam, *J. Heat Transfer, Proc. 5th Int. Heat Transfer Conf.*, 1, 83 (1974).

6. V. S. Arpaci, *Int. J. Heat Mass Transfer,* **11**, 871 (1968).
7. R. D. Cess, *J. Heat Transfer*, **86**, 469 (1964).
8. J. L. Novotny, J. R. Lloyd, and J. D. Bankston, *Progr. Astr. Aeronaut.*, **39**, 309 (1975).
9. C. L. Tien and J. E. Lowder, *Int. J. Heat Mass Transfer*, **9**, 698 (1966).
10. Y. Yamada, *Int. J. Heat Mass Transfer,* **31**, 429 (1988).
11. W. Malkmus, *J. Opt. Soc. Am.*, **57**, 323 (1967).
12. A. Soufiani, J. M. Hartmann, and J. Taine, *J. Quant. Spectrosc. Radiat. Transfer,* **31**, 243 (1985).
13. M. Cherkaoui, *Modélisation et étude de sensibilité des échanges radiatifs et conductifs couplés dans l'air ambiant*, Ph.D. Dissertation, Universite Paris XII, France (1993).
14. J. Liu and S. N. Tiwari, *ASME HTD,* **244**, 21 (1993).
15. S. S. Penner, *Quantitative Molecular Spectroscopy and Gas Emissivities*, Pergamon, London, **6**, 199 (1959).
16. C. L. Tien, *Advances in Heat Transfer,* Academic Press, New York, **5**, 254 (1968).
17. S. J. Young, *J. Quant. Spectrosc. Radiat. Transfer*, **18**, 1 (1977).
18. J. R. Howell, in: T. F. Irvine and J. P. Hartnett (eds.), *Advances in Heat Transfer*, **1** (1968).